

ABSORPTION SATURATION IN THE ELECTRON-PHONON SPECTRUM OF CdSe

A. F. DITE, V. B. TIMOFEEV, V. M. FAÏN, and É. G. YASHCHIN

Institute of Solid State Physics, U.S.S.R. Academy of Sciences

Submitted July 25, 1969

Zh. Eksp. Teor. Fiz. 58, 460-474 (February 1970)

The dependence of the absorption coefficient in the exciton-phonon spectrum of semiconductors on the intensity of the incident monochromatic radiation is analyzed theoretically. Two possible absorption saturation mechanisms are considered. One, which may be termed an integral mechanism, occurs with conservation of the nonequilibrium exciton distribution in the band and when the intraband relaxation is more rapid than the departure of excitons from the band. The second, so-called differential saturation mechanisms, is characterized by a nonequilibrium distribution of excitons in the band and takes place if the rate of exciton departure from any point of the band is greater than the rate of intraband relaxation. A Q-switched ruby laser was used to study the nonlinear absorption in the exciton-phonon spectrum of CdSe single crystals at 80-120°K. The integral saturation mechanism is found to occur. The mean exciton lifetimes in the band are found; in the indicated temperature range they vary between 10⁻⁸ and 3 × 10⁻⁹ sec.

THE possibility of saturating the absorption of incident radiation in the exciton-phonon spectrum of semiconductors (indirect optical transitions) was indicated in an earlier paper,^[1] where theoretical estimates were presented for this phenomenon and the connection between it and possible parametric generation of excitons and phonons in the semiconductor was established. The present paper is devoted to observation of saturation in the region of the exciton-phonon absorption spectrum in CdSe crystals.^[1]

1. THEORY OF ABSORPTION SATURATION IN EXCITON-PHONON SPECTRA OF SEMICONDUCTORS

1. Before we proceed to describe the experiment, we present a detailed theoretical analysis of the effect of saturation in indirect exciton-phonon transitions in semiconductors.

We shall deal henceforth with the dependence of the absorption coefficient on the power flux incident on the crystal. The absorption takes place in a section of the exciton-phonon spectrum, characterized by the conservation laws

$$\hbar\omega = E_g - G + \mathcal{E}(k) - \hbar\Omega(-k), \tag{1}$$

where ω is the radiation frequency, E_g the width of the forbidden band, G the exciton binding energy, Ω the frequency of the optical phonon, and $\mathcal{E}(k)$ for an exciton band with an extremum at $k = 0$ is equal to

$$\mathcal{E}(k) = \hbar^2 k^2 / 2m. \tag{2}$$

Here $\hbar k$ is the quasimomentum of the exciton, and $m = m_e + m_h$ is the exciton mass. The change of the number of excitons $n(k)$ and phonons $\nu(k)$ per unit time

(and per unit volume) under the influence of the incident flux of radiation P (power through a unit area) and the relaxation processes can be written in the form

$$\dot{n}(k) = I[n(k)] - w(k, \omega)P(\omega)[n(k) - \nu(-k)] - \gamma_{ex}(k)n(k), \tag{3}$$

$$\dot{\nu}(k) = -\gamma_{ph}(k)[\nu(k) - \nu_0] + w(k, \omega)P(\omega)[n(k) - \nu(-k)]. \tag{4}$$

Here $I[n(k)]$ is the collision integral, which takes into account the intraband transitions, particularly the collisions between the exciton and the acoustic phonons, $\gamma_{ex}(k)$ is the reciprocal lifetime of an exciton with momentum $\hbar k$ in the exciton band, $\gamma_{ph}(k)$ the reciprocal lifetime of the phonon, ν_0 the equilibrium number of phonons, and $w(k, \omega)$ a function characterizing the probability of the transitions under the influence of the radiation. It is easy to show that the function $w(k, \omega)$ is connected with the absorption coefficient α in the following manner:

$$\alpha = \hbar\omega \sum_k w(k, \omega)(\nu - n). \tag{5}$$

In a weak field, when the number of excited excitons can be assumed equal to zero, the absorption coefficient does not depend on P and is equal to

$$\alpha_0 = \hbar\omega \nu \sum_k w(k, \omega). \tag{6}$$

We shall henceforth neglect the dispersion—the k -dependence of the quantities pertaining to the optical phonon of frequency Ω . In addition, we shall use the approximation of spherically-symmetrical bands. In this case w depends on the absolute value $|k| = k$ and, recognizing that w is proportional to the probability per unit time, we can represent in the form

$$w(k, \omega) = A(k) \frac{\sigma}{\pi\hbar} \left\{ \left[\frac{E_g - G + \mathcal{E}(k) - \Omega - \omega}{\hbar} \right]^2 + \sigma^2 \right\}^{-1} \approx A(k) \delta[E_g - G + \mathcal{E}(k) - \hbar\Omega - \hbar\omega], \tag{7}$$

where σ is equal to the sum of the line widths of the exciton $\mathcal{E}(k)$ and of the phonon Ω . The quantity $A(k)$ can be expressed in terms of the effective dipole mo-

¹Nonlinear absorption was observed earlier in spectra of mixed CdS_{0.1}Se_{0.9} crystals dissolved in a glass matrix (type KS-19 glass) [2,3]. Such objects have an imperfect polycrystalline structure, in which there are no exciton spectra, and therefore the saturation of the absorption in them has a nature which apparently is not connected with excitons.

ment $D(\mathbf{k})$ with the aid of the relation

$$A(k) = \frac{4\pi^2}{\hbar c} D^2(k). \quad (8)$$

Going over in (6) from summation with respect to \mathbf{k} to integration with respect to the energy (2), and using (7), we obtain

$$\alpha_0 = A(\mathcal{E}) \frac{m^{3/2} \sqrt{\mathcal{E}} \omega v}{\sqrt{2\pi^2 \hbar^2}},$$

and for the dipole moment

$$D^2(\mathcal{E}) = \frac{\hbar^3 c \alpha_0}{2^{3/2} m^{3/2} v \sqrt{\mathcal{E}} \omega v}. \quad (9)$$

2. To determine the dependence of the absorption coefficient on the power flux P , it is necessary to find the dependence of the quantity $(n - \nu)$ on P . We then obtain with the aid of (5) the dependence of α on P . The dependence of $(n - \nu)$ on P can be determined from Eqs. (3) and (4). We shall further consider the stationary case $\dot{n} = \dot{\nu} = 0$. This means that we assume the action of the light source (laser) to be sufficiently long compared with all the characteristic relaxation times. In solving Eqs. (3) and (4), we use averaging over the angles and consider two limiting cases:

a) the intraband relaxation described by the term $I(n)$ is faster than the departure of the excitons from the band

$$|I(n)| \gg \gamma_{ex} n, \quad (10)$$

b) the intraband relaxation is slower than the departure from the band, i.e.,

$$|I(n)| \ll \gamma_{ex} n. \quad (11)$$

We consider first the case (a) (condition (10)). To be specific, we take into account the relaxation inside the exciton band (near its center) due to the collisions between the excitons and the acoustic phonons. From the conservation laws it follows that the exciton momentum can change appreciably in direction in each individual act of collision with the phonon, but the change of the exciton energy (in a sufficiently wide interval of energies $\mathcal{E}(k)$) is smaller if $(\mathcal{E} m s^2)^{1/2} \ll kT$, where s is the speed of sound (almost elastic collision). This means that the exciton energy relaxation (the so-called thermalization of the excitons) is much slower than the momentum relaxation. Thus, if $\tau(\mathcal{E})$ is the average lifetime in a state with wave vector $\mathbf{k}(\mathcal{E})$, then the average exciton energy relaxation time in an interval of the order of kT is (see for example, ⁽⁴⁾)

$$\bar{\tau}(\mathcal{E}) = \frac{kT}{2ms^2} \tau(\mathcal{E}). \quad (12)$$

We assume further that the second term on the right side of (3) is small compared with the first. It is easy to show that this means that

$$|E|^2 |D|^2 \hbar \bar{\tau} / kT \ll 1, \quad (13)$$

where $|E|$ is the modulus of the electric-field vector. At the same time, condition (10) can be rewritten in the form

$$1 / \bar{\tau} \gg \bar{\gamma}_{ex}. \quad (14)$$

²⁾The cited literature considers electron relaxation processes but it is easy to see that the entire reasoning can be used without change for excitons.

Under these conditions it can be assumed that the excitons are in quasiequilibrium in the band with $n = C \exp(-\mathcal{E}/kT)$. The constant C , and by the same token the absorption coefficient (from (5)), can be determined from

$$\sum_{\mathbf{k}} w(k, \omega) P(\nu - n) = \sum_{\mathbf{k}} \gamma_{ex}(\mathbf{k}) n(\mathbf{k}), \quad (15)$$

which is obtained in the stationary case as a result of summation of (3), with $\sum_{\mathbf{k}} I[n(\mathbf{k})] = 0$, since the total number of excitons is conserved in intraband collision processes. As a result we obtain

$$\alpha = \alpha_0 / (1 + f_1 P), \quad (16)$$

where

$$f_1 = \frac{\alpha_0 \exp[-\mathcal{E}_0/kT]}{v \hbar \omega \Gamma}. \quad (17)$$

Here \mathcal{E}_0 is the value of \mathcal{E} determined from the conservation law (1) and

$$\Gamma = \sum_{\mathbf{k}} \exp\left[-\frac{\mathcal{E}(\mathbf{k})}{kT}\right] \gamma_{ex}(\mathbf{k}). \quad (18)$$

We now proceed to consider case (b) (condition (11)). We note immediately that the condition (11) for intraband relaxation due to collisions with acoustic phonons takes the form

$$\bar{\tau}^{-1} \ll \gamma_{ex}. \quad (19)$$

In this case the system (13)–(14) under stationary conditions can be written in the form

$$(wP + \gamma_{ex})n = wP\nu, \quad (\gamma_{ph} + wP)\nu - wPn = \gamma_{ph}\nu_0.$$

Solving these equations, we obtain

$$\nu - n = \nu_0 \left(1 + \frac{wP(\gamma_{ph} + \gamma_{ex})}{\gamma_{ph}\gamma_{ex}}\right)^{-1}. \quad (20)$$

Substituting this expression and (7) in (5), we obtain

$$\alpha = \hbar \omega \nu_0 \sum_{\mathbf{k}} A(k) \left[\frac{1}{\pi \hbar [(E_g - G + \mathcal{E})/\hbar - \Omega - \omega]^2 + \sigma^2 (1 + f_2 P)} \right] \times \frac{1}{\sqrt{1 + f_2 P}}.$$

Approximating the expression in the square brackets by a δ -function, we obtain

$$\alpha = \alpha_0 / \sqrt{1 + f_2 P}, \quad (21)$$

where³⁾

$$f_2 = \frac{\pi \hbar \alpha_0 \sqrt{2}}{m^{3/2} \omega v \sqrt{\mathcal{E}} \gamma_{ph} \gamma_{ex}}. \quad (22)$$

Thus, there are two possible saturation mechanisms in the exciton-phonon spectrum. In the first mechanism, described by formulas (16) and (17), the saturation occurs with the quasiequilibrium of the excitons in the band conserved, and is determined by the balance between the influx of electrons into the band, due to radiation, and the departure from all the points of the band. This departure is characterized by the averaged probability (18) and therefore does not depend on the exciton

³⁾A factor of the form $(\gamma_{ex} + \gamma_{ph})/\sigma$ has been omitted from (22), since $\sigma = \gamma_{ph} + \gamma_{ex}$ if Lorentz contours are assumed for the exciton and phonon lines.

wave vector. We shall henceforth call this the integral saturation mechanism. It can come into play if the relaxation of the electrons inside the band is faster than their departure from the band. This mechanism corresponds in radio spectroscopy to saturation in a homogeneously broadened line. The entire exciton band enters here as a single level, with a broadening characterized by Γ .

The other mechanism, described by formula (21) and (22), is determined by the balance between the influx of excitons due to radiation and the departure of excitons from a given point of the band under the assumption that this departure is faster than the establishment of quasi-equilibrium in the band (condition (19)). The saturation parameter f_2 in this mechanism is determined by the quantity $\gamma_{\text{ex}}(\mathbf{k})$, which characterizes the departure from the given point of the band. We shall call this the differential mechanism. It corresponds in radio spectroscopy to saturation in an inhomogeneously broadened line.

It is of interest to estimate the possibility of saturation in either case in terms of the matrix element of the indirect transition D and the relaxation times. It is easy to obtain the saturation condition (when condition (13) is fulfilled) in the form

$$\frac{|D|^2|E|^2}{\hbar^2 \bar{\gamma}_{\text{ex}} kT/\hbar} \sim 1, \quad \bar{\tau} \ll \bar{\gamma}_{\text{ex}}^{-1} \quad (23)$$

for the integral mechanism (where $\bar{\gamma}_{\text{ex}}$ is the average value of $\gamma_{\text{ex}}(\mathbf{k})$) and

$$\frac{|D|^2|E|^2}{\hbar^2 \gamma_{\text{ex}}(k) \gamma_{\text{ph}}} \sim 1 \quad (24)$$

for the differential mechanism. In both cases it is assumed that

$$\gamma_{\text{ph}} \gg \gamma_{\text{ex}}.$$

We see that the condition of integral saturation (23) is more stringent if $kT/\hbar \gg \gamma_{\text{ph}}$, which is usually the case for temperatures on the order of 100°K . On the other hand, however, for differential saturation to be possible it is necessary that no quasiequilibrium in the band be established as a result of the intraband processes; in concrete situations this may not be the case. We note also that in the differential saturation mechanism, a non-equilibrium distribution of the number of excitons, described by expression (20), is established.

In concluding this section, we note that the most favorable objects of investigation of these phenomena, from the point of view of experiment, are wurtzite semiconducting crystals of the II-VI group, in which exciton-phonon transitions take place in the center of the Brillouin zone (near the Γ point) as a result of the interaction of the excitons with the L_0 phonons. The moments of the exciton-phonon transitions in such crystals greatly exceed the corresponding moments for crystals in which "oblique" exciton-phonon transitions takes place, and therefore, in accordance with conditions (23) and (24), absorption saturation sets in at much lower values of the incident-radiation power flux. This difference is determined mainly by the fact that in second order of perturbation theory the moment of the exciton-phonon transition has the square of the energy denominator, containing the difference between the energies

the intermediate (virtual) and final states of the exciton. The ratio of the moments, with CdS crystals as an example (the exciton phonon transitions are vertical, in the center of the Brillouin zone) and Si (oblique exciton-phonon transitions) is $\sim 10^2$.

As the experimental objects we chose hexagonal CdSe crystals, being the most convenient because at suitable crystal temperatures the ruby-laser radiation falls in the region of the long-wave edge of the fundamental absorption.

2. EXPERIMENTAL PROCEDURE

1. We used CdSe single crystals grown by the Piper method from the gas phase. We selected for the investigations the most perfect crystals from the point of view of stoichiometric composition and minimum impurity contents, whose spectra contained no discrete structure due to the bound exciton states (at $T = 77.3^\circ\text{K}$ and above).

Plane-parallel plates 2–0.2 mm thick were cut from the single-crystal blocks in such a way that the hexagonal c axis was in the plane of the working face ($(10\bar{1}0)$ plane). To exclude henceforth the influence of the surface layer, which is damaged by mechanical working, the CdSe plates were chemically polished in a solution $7\text{K}_2\text{CrO}_7 + 3\text{H}_2\text{SO}_4$ (layer dissolution rate $\sim 5 \mu/\text{min}$). The quality of the optical surfaces processed in this manner was monitored against the reflection spectra in the region of the discrete exciton structure, and also against the edge absorption spectrum, and was compared with the corresponding spectral properties of natural surfaces (cleaved surfaces or natural growth faces).

2. The spectral distribution of the absorption coefficient (the linear absorption coefficient) was measured in polarized light using a single-beam prism spectrometer based on the ISP-51 spectrograph with a UF-90 camera. The spectral resolution in the working region was not worse than 0.001 eV. The absorption coefficients α were calculated from the transmission curves by means of a formula that takes into account multiple reflections in the sample (this is significant in the region where $\alpha l \sim 1$):

$$\alpha = \frac{1}{l} \ln \left[\frac{(1-R)^2}{2T} + \sqrt{\frac{(1-R)^4}{(2T)^2} + R^2} \right],$$

where l is the sample thickness, R the reflection coefficient, and T the optical density.

The samples were placed in a specially constructed cryostat, in which provision was made for fastening them without possible deformation during the course of cooling. The temperature in the cryostat could change in the interval $77\text{--}300^\circ\text{K}$ and was monitored with accuracy $\sim 1^\circ\text{K}$.

3. The absorption saturation was measured with an experimental setup whose block diagram is shown in Fig. 1. The radiation source was a Q-switched ruby laser (radiation power density $\sim 20 \text{ MW}/\text{cm}^2$, single-pulse duration $\sim 15\text{--}20 \text{ nsec}$). The Q-switch was a passive shutter based on an alcohol solution of cryptocyanine. The radiation of the laser was focused with a lens L on a crystal placed in the cryostat. Part of the radiation was diverted with the aid of a plane-parallel plate P to

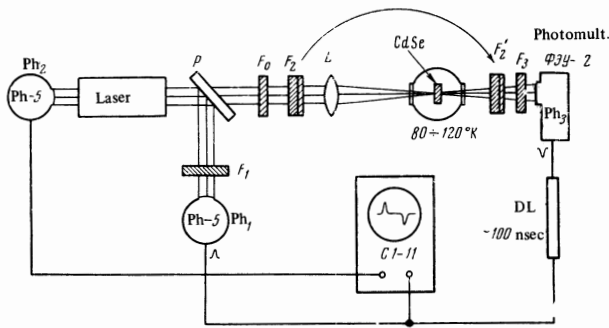


FIG. 1. Block diagram of experimental setup for the study of absorption saturation.

a power-calibrated photodetector Ph₁, for the purpose of monitoring the power and the duration of the light pulse from the laser. The radiation from the crystal was fed to photomultiplier Ph₃, which was also power-calibrated beforehand. The signal from the photomultiplier was fed through a delay line DL to a high-speed pulsed oscilloscope S-11 simultaneously with the reference signal from Ph₁. The oscilloscope operated in the external-synchronization mode with the aid of a signal from the detector Ph₂. The time constant of the entire registration system was ~ 10 nsec.

The laser pulse directed to the crystal was attenuated with a system of calibrated filters F₂. By shifting the filters F₂ from the input to the output of the crystal, which maintained the total attenuation of the light going to the photomultiplier Ph₃ constant, it was possible to control the radiation power flux from the laser at the input of the crystal.

The error in the distribution of the absolute values of the powers did not exceed a factor of 2. The relative measurements of the signals P₀ and P were made with accuracy $\sim 20\%$. In measurements of the powers of the light signals at the input and output of the crystal, care was taken to ensure linear operation of the photodetectors Ph₁ and Ph₃. The radiation power density incident on the crystal ranged from 10^2 to 5×10^7 W/cm². In this range of power, the transmission of the CdSe crystals changed appreciably (by almost three orders of magnitude). Therefore, in order to compensate for the strong change of the transmission of the crystals, additional calibrated filters F₃ were placed ahead of the photomultiplier.

Figure 2 shows oscillograms illustrating the nonlinear absorption of the CdSe crystals. On each of the oscillograms, the first pulse (upward from the sweep line) is proportional to the power at the input of the crystal, and the second is connected with the signal past the crystal. At $E \perp c$, the change of the transmission of the



FIG. 2. Oscillograms of the process of absorption saturation for $E \perp c$: a - P₀ 250 W/cm², b - P₀ 6.2 kW/cm², c - P₀ 22.5 kW/cm².

CdSe is appreciable, and begins already at relatively low powers. In the case of a polarization $E \parallel c$, the absorption of CdSe changes insignificantly in the range $1-10^6$ kW/cm². Nevertheless, the presence of a certain decrease of absorption at very high powers (~ 1 MW/cm² and above) is apparently connected with inaccurate orientation of the crystal in the case of $E \parallel c$.

3. EXCITON PHONON ABSORPTION SPECTRUM OF CdSe

In spite of the appreciable number of experimental investigations devoted to the structure of the energy bands of hexagonal CdSe crystals, and also to the character of the optical transitions between the extremal points of the bands (see, for example, [5-9]), the nature of the long-wave edge of the fundamental absorption of these crystals is still unclear.

In an investigation of the edge of the intrinsic absorption spectrum, Konak, Dillinger, and Prosser [10] pointed out the strong influence exerted on the form of the CdSe spectrum by the impurity states located near the nearest extremum of the conduction band. The authors of [10] were unable to separate the exciton absorption in which phonons take part. To be sure, in a later investigation they noted singularities in the intrinsic-reflection spectra, and attributed these singularities to exciton-phonon transitions in band A, with emission of L0 phonons.

The edge absorption spectrum of mixed CdS_{0.1}Se_{0.9} crystals dissolved in a glass matrix (type KS-19 glass) was interpreted in [2] on the basis of the concept of oblique electron-phonon transitions. It must be noted here, however, that the values of the phonon energies obtained in [2] do not agree with the values obtained directly from the IR reflection spectra. In addition, the values given in [2] for the width of the forbidden band are too low.

At the same time, Segal [12] called attention to the fact that a common feature of the structure properties of hexagonal semiconducting crystals of the II-VI group is that the nearest extrema of the valence and conduction bands lie at the point $k = 0$ (the Γ point). He emphasized the appreciable role of the absorption processes as a result of exciton transitions with absorption of L0 phonons, which were previously observed in a number of crystals of the II-VI group. [13-15]

In connection with the foregoing, we deemed it advisable to perform detailed measurements of the form and of the temperature dependence of the long-wave edge of the intrinsic-absorption spectrum of CdSe crystals.

Figure 3 shows the spectral distribution of the absorption coefficient at low temperatures for a light polarization $E \perp c$ in terms of the coordinates $\sqrt{\alpha}$ and $\hbar\omega$. The arrows on the lower right of this figure indicate the positions, on an energy scale, of the lowest exciton state (exciton band A, $n = 1$), determined from the reflection spectra at the same temperatures. It is easy to note the linear sections of the plots of $\sqrt{\alpha}$ against $\hbar\omega$. Continuing the linear sections of the curves until they cross the abscissa axis, we see that the points of intersection are located 0.027 ± 0.002 eV from the corresponding positions of the exciton peaks. Consequently, the intrinsic absorption sets in already in the spectrum section located at a distance 0.027 eV (the "red"

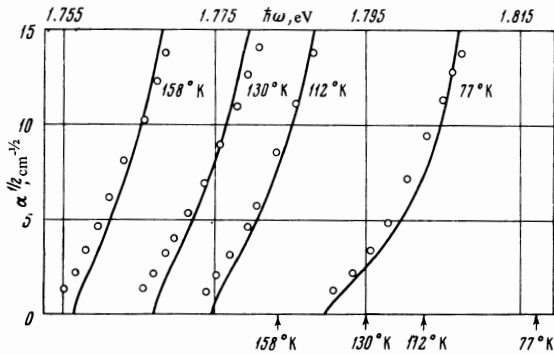


FIG. 3. Spectral distribution of the absorption coefficient in the exciton-phonon spectrum at temperatures 77, 112, 130, and 158°K.

boundary) from the region of the direct transitions to the lowest exciton band A. We note that within the limits of experimental errors, this value corresponds to the energy of the LO phonon in the CdSe lattice.^[16] The slope of the linear section of the curves of Fig. 3 decreases with decreasing temperature, in qualitative agreement with the process of the "freezing out" of the phonons when the crystals are cooled. Thus, the results presented above offer evidence that the optical phonons play an important role in the exciton absorption in CdSe crystals.

The theory of exciton absorption, with participation of optical phonons as a result of vertical transitions in the center of the Brillouin zone was developed in^[13, 12].⁴⁾ The process of absorption of a photon $\hbar\omega$ with simultaneous absorption of an LO phonon $\hbar\Omega(\mathbf{k})$ and production of an exciton $\mathcal{E}(-\mathbf{k})$ satisfies conservation laws of the type (1).

The corresponding process of excitation of the excitons in the case of intraband scattering is illustrated in Fig. 4.

The matrix element of the exciton-phonon interaction in the case of an interaction with optical phonons is proportional to $|\mathbf{k}|$ for small \mathbf{k} (we have in mind the scattering of excitons in the center of the band without a change of the internal quantum number). If the dispersion in the exciton band is quadratic, we obtain for the absorption coefficient in the exciton-phonon spectrum a distribution (in the second order of perturbation theory) in the form

$$\alpha = \alpha_0 \frac{\mathcal{E}^{3/2}}{(\mathcal{E} - \hbar\Omega)^2} \nu, \quad (25)$$

where \mathcal{E} is the energy of the exciton in the band and ν is the occupation number of the LO phonon at $\mathbf{k} = 0$ (we neglect the phonon dispersion).

It was of interest to compare the experimentally observed temperature and frequency dependences of the absorption coefficients with the theoretical result (expression (25)). The results of such a comparison are shown in Fig. 3, where the points correspond to the experiment, and the solid curves are the result of an approximation with the aid of expression (25) at the experimental value of the parameter $\alpha_0 = 2 \times 10^5 \text{ cm}^{-3/2}$.

⁴⁾The first to consider the processes of absorption in vertical transitions, with participation of optical phonons, was Dumke^[17], but he considered the case of electron-phonon absorption.

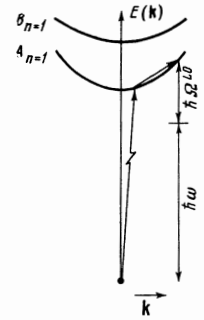


FIG. 4. Energy diagram of the exciton-phonon transition with absorption of LO phonon. The scattering of the exciton takes place inside the exciton band A.

On the whole, the theoretical approximation (25) describes the temperature and spectral properties of the absorption curve satisfactorily. Discrepancies are observed in the region of the longest-wavelength boundary, where the spectrum is somewhat smeared out, particularly when the temperature is increased. An analogous smearing of the edges of the exciton-phonon spectrum was observed in crystals of Ge, Si^[18] and Cu₂O,^[19] and is obviously connected with processes of exciton scattering by acoustic phonons (the attenuation processes are not taken into account in expression (25)). Nor is it excluded that at higher temperatures ($T \sim 300^\circ\text{K}$) the processes of absorption with participation of two or more phonons become important, leading to a smearing of the spectrum.

Thus, the long-wave edge of the intrinsic absorption spectrum in CdSe single crystals can be interpreted as the result of exciton transitions at the center of the band, with participation of optical phonons. This result is the consequence of the common structural properties of hexagonal semiconducting crystals of the II-VI group.

4. ABSORPTION SATURATION IN THE EXCITON-PHONON SPECTRUM OF CdSe

Our aim was to investigate the dependence of the exciton-phonon absorption on the power of monochromatic radiation incident on the crystal, in different regions of the exciton-phonon spectrum. Since we had at our disposal a coherent source with stable frequency ($\hbar\omega = 1.786 \text{ eV}$), we used for our task the temperature shift of the edge spectrum of the intrinsic absorption.⁵⁾

Measurements of the nonlinear absorption in the exciton-phonon spectrum were made at $T = 80\text{--}120^\circ\text{K}$, corresponding to an energy shift $\sim 0.012 \text{ eV}$ in the exciton band and to the range of wave vectors $|\mathbf{k}|$ from 2.3×10^6 to $7 \times 10^6 \text{ cm}^{-1}$. The choice of the lower value of the temperature is limited by the red boundary of the exciton-phonon spectrum (at $\hbar\omega < E_g - G + \mathcal{E}(\mathbf{k}) - \hbar\Omega$, the laser emission lies in the transparency region of the CdSe crystals). At $T \sim 120^\circ\text{K}$, the radiation falls in the spectral region where direct transitions to the exciton band A already appear, so that the approximation of the form of the spectrum with the aid of expression (25) becomes meaningless in this region.

⁵⁾The temperature shift of the exciton band A relative to the ground state of the crystals in the temperature region $\sim 80^\circ$ is $\partial\mathcal{E}/\partial T = 4.1 \times 10^{-4} \text{ eV/deg}$ (see also [9]). The temperature shift was monitored against the location of the line A in the reflection spectrum.

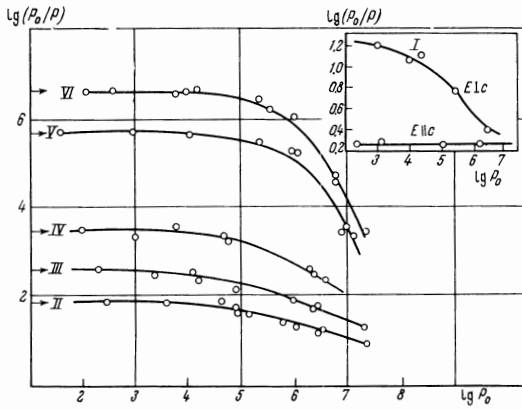


FIG. 5. Dependence of the optical density in the exciton-phonon spectrum region on the radiation power flux (P_0 in W/cm^2) at the input to the crystal. The curves correspond to the following temperatures ($^{\circ}\text{K}$): VI – 129, V – 121, IV – 110, III – 104, II – 100, I – 80.

Figure 5 shows the dependence of the optical density of the CdSe crystals on the radiation power incident on the crystal, in coordinates $\log(P_0/P)$ and $\log P_0$. Each of the curves corresponds to exciton-phonon transitions to different sections of the exciton band (the value of $\mathcal{E}(k)$ increases with increasing number of the curve). The upper limit of the power of the plots shown in Fig. 5 is connected with the mechanical damage to the crystals, which sets in at $P \sim 5 \times 10^7 \text{ W}/\text{cm}^2$. The arrows along the ordinate axis indicate the limiting values of the optical densities at zero power $P_0 = 0$. Attention should be called to the fact that a noticeable decrease of the absorption sets in already at relatively low values of the powers at the input ($P_0 \sim 10^4 \text{ W}/\text{cm}^2$). Practically complete saturation could be observed only in the longest-wavelength part of the exciton-phonon spectrum ($E \perp c$, see curve I in Fig. 5 in the upper right corner). The absorption for the polarization $E \parallel c$ ("phonon" absorption) is practically independent of the power. We note that working with a radiation power on the order of $1 \text{ MW}/\text{cm}^2$ and above, local heating of the crystal by as much as 1° or more can take place, and this can affect the measured absorption. Therefore in all the following discussions of the nonlinear properties of the exciton-phonon absorption we use results obtained at $P_0 < 1 \text{ MW}/\text{cm}^2$.

5. DISCUSSION OF RESULTS

It was of interest to consider analytically the change of the optical density of the exciton-phonon spectrum as a function of the radiation power P_0 incident on a crystal of thickness l , and then compare the result with experiment. To this end, we use the already known (Sec. 1) regularities of nonlinear absorption in the case of the integral and differential saturation mechanisms.

The analysis reduces to a solution of an integral equation in the form

$$l = \int_P^{P_0} \frac{dP}{P\alpha(P)}, \quad (26)$$

in which $\alpha(P)$ should be replaced by the explicit expression (16) or (21), depending on the saturation mechanism. Equation (26) does not take into account multiple reflections of the light in the crystal, a procedure

valid when applied to the discussed experiment, since $\alpha l > 1$ under the conditions of this experiment. Using an asymptotic approximation of the type $(\alpha l - \ln(P_0/P)) \ll 1$, corresponding to the region where the absorption depends little on the power, we obtain an expression for the saturation parameters f_1 and f_2 in the cases of integral and differential mechanisms, in the form

$$f_1 = \frac{\alpha_0 + \alpha_1}{\alpha_0(P_0 - P)} \left(\alpha l - \ln \frac{P_0}{P} \right) = \frac{1}{2} f_2, \quad (27)$$

where α_0 and α_1 are the exciton-phonon and "phonon" absorption coefficients, and P is the radiation power at the output of the crystal. Solving Eq. (26), we can easily obtain the connection between the powers P_0 and P , the saturation parameters f_1 or f_2 , and the absorption coefficients α_0 and α_1 . The corresponding expressions for the differential and integral mechanisms, represented in the form of invariants, are

$$\left[\frac{2\alpha_0^2}{\alpha(\alpha_0^2 - \alpha_1^2)} \ln(\alpha_1 x + \alpha_0) + \frac{1}{\alpha_0 + \alpha_1} \ln(x-1) - \frac{1}{\alpha_0 - \alpha_1} \ln(x+1) \right] \Big|_x^{x_0} = l, \quad (28)$$

$$\left[\frac{\alpha_0}{(\alpha_0 + \alpha_1)\alpha_1} \ln(\alpha_1 + \alpha_0) + \frac{1}{\alpha_1 + \alpha_0} \ln(x-1) \right] \Big|_x^{x_0} = l, \quad (28')$$

where in (28)

$$x_0 = \sqrt{1 + f_2 P_0}, \quad x = \sqrt{1 + f_2 P},$$

and in (28')

$$x_0 = 1 + f_1 P_0, \quad x = 1 + f_1 P.$$

We have attempted to ascertain which of the saturation mechanisms is realized in our case. To this end, we used (27) to calculate the values of the saturation parameters f_1 and f_2 for each of the curves of Fig. 5 (we used the dependence of the optical density on the power in the region of the weak nonlinearity in accordance with the asymptotic approximation). We then verified the invariants of expressions (28) and (28') using the experimentally obtained values of the optical transmission of the crystals in the entire range of powers P_0 .

The calculations performed in this manner have shown that it is difficult to draw any definite conclusions concerning the saturation mechanism, although good agreement between theory and experiment takes place in the case of the integral saturation mechanism. The point is that in expressions (28) and (28'), which have an integral character, the significant difference between relations (16) and (21) becomes leveled out (these equations have a local meaning, i.e., for each point of the crystal). Therefore, owing to the low accuracy in the determination of the absolute values of the powers (by an approximate factor of 2), we were unable to establish the saturation character uniquely in this manner.

To ascertain the saturation mechanism, we investigated additionally the spectrum of the exciton luminescence, which was excited with a ruby laser in the exciton-phonon region of the absorption spectrum. Under the conditions of strong absorption saturation at the location of the exciton band (for example, at $|\mathbf{k}_0|$), where the optical transition is completed, the occupation numbers of the excitons and of the phonons actually become equalized, $n(\mathbf{k}_0) \rightarrow \nu(\mathbf{k}_0)$. If at the same time the exciton energy relaxation is slower than their departure from

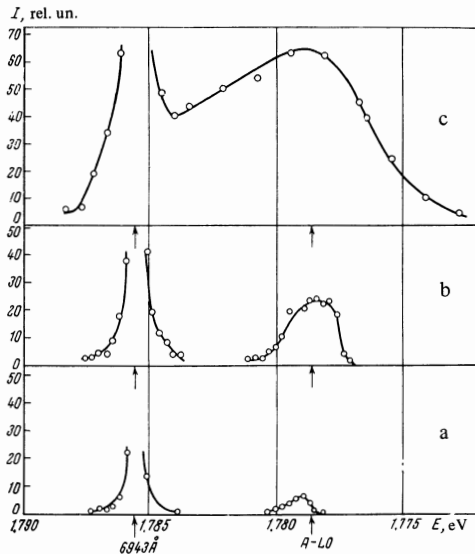


FIG. 6. Intensity distribution in exciton-phonon luminescence excited by a ruby laser ($\lambda = 6943 \text{ \AA}$) at powers $2 \times 10^6 \text{ W/cm}^2$ (a), 10^7 W/cm^2 (b), and $5 \times 10^7 \text{ W/cm}^2$ (c). The arrows indicate the positions of the red boundary of the exciton-phonon spectrum (A - L0) and of the laser line.

$\bar{\nu}(k, \text{eV})$ ($T, \text{ }^\circ\text{K}$)	$\bar{\nu}_{\text{ex}} \cdot 10^{-4}$	$\bar{\tau}_{\text{ex}} \cdot 10^8$	f_1	$\bar{\nu}(k, \text{eV})$ ($T, \text{ }^\circ\text{K}$)	$\bar{\nu}_{\text{ex}} \cdot 10^{-4}$	$\bar{\tau}_{\text{ex}} \cdot 10^8$	f_1
0.0048 (100)	1.08	9.25	$1.1 \cdot 10^{-2}$	0.0134 (121)	1.57	6.4	$5 \cdot 10^{-3}$
0.006 (104)	1.1	9.1	$1 \cdot 10^{-2}$	0.0166 (129)	1.9	5	$3.54 \cdot 10^{-3}$
0.0087 (110)	1.12	9.0	$0.9 \cdot 10^{-2}$				

In the case of the integral mechanism, the saturation parameter f_1 can be related to the average lifetime of the exciton in the band $\bar{\tau}_{\text{ex}} = \bar{\nu}_{\text{ex}}^{-1}$ (see (17)). We can readily see that

$$\bar{\nu}_{\text{ex}} = \Gamma / \sum_k e^{-\bar{\nu}(k)/kT}$$

The table lists the values of the parameters f_1 determined from the curves on Fig. 5 and from formula (27), and also the values of $\bar{\nu}_{\text{ex}}$ and $\bar{\tau}_{\text{ex}}$, calculated with the aid of expressions (17) and (29). The tabulated data reveal a certain temperature dependence of the average lifetimes of the excitons in the band. As expected, when the temperature is increased a monotonic decrease of these times is observed.

We note that in the differential mechanism of saturation it is possible to determine the lifetimes $\nu_{\text{ex}}^{-1}(k)$ at each point of the exciton band.

Thus, an investigation of the saturation of the absorption in the exciton-phonon spectrum of the semiconductors is a method for investigating the kinetics of the excitons. On the other hand, the investigation can be useful in the experimental solution of the problem of parametric generation of quasiparticles—excitons and phonons.

The authors are grateful to I. B. Levinson and É. I. Rashba for useful discussions.

¹ V. Faïn, Zh. Eksp. Teor. Fiz. 53, 2070 (1967) [Sov. Phys.-JETP 26, 1171 (1968)].

² A. M. Bonch-Bruevich, T. K. Razumova, and G. M. Rubanova, Proc. (Trudy) Second All-union Symp. on Nonlinear Optics, Novosibirsk, 1968.

³ A. M. Bonch-Bruevich, T. K. Razumova, and G. M. Rubanova, Fiz. Tverd. Tela 9, 2265 (1967) [Sov. Phys.-Solid State 9, 1623 (1968)].

⁴ P. A. Kazlauskas and I. B. Levinson, Litovsk. fizich. sbornik (Lithuanian Phys. Collection) 6, 33, 233 (1966).

⁵ J. O. Dimmock and R. G. Wheeler, J. Appl. Phys. 32, 2271 (1961).

⁶ R. B. Parsons, W. Wardsinski, and A. D. Joffe, Proc. Roy. Soc. A262, 120 (1961).

⁷ V. V. Sobolev, Dokl. Akad. Nauk SSSR 152, 1342 (1963) [Sov. Phys.-Dokl. 8, 996 (1964)].

⁸ V. V. Sobolev, ibid. 165, 534 (1965) [10, 1085 (1966)].

⁹ V. V. Sobolev, Opt. Spektr. 16, 76 (1964).

¹⁰ C. Konak, J. Dillinger, and V. Prosser, II-VI Semicond. Compounds Intern. Conf. N. Y. 1967, p. 850.

¹¹ J. Dillinger, C. Konak, V. Prosser, J. Sak, and M. Svava, Phys. Stat. Sol. 29, 707 (1968).

¹² B. Segall, Phys. Rev. 163, 769 (1967); 150, 734 (1966).

¹³ D. G. Thomas, J. J. Hopfield, and H. Power, Phys.

the band (the differential saturation mechanism), then the inequality $n(k) < \nu(k_0)$ is satisfied at any point of the band, and the exciton-phonon luminescence has a spontaneous character. On the other hand, if under the conditions of strong saturation of the absorption the exciton energy relaxation is the faster process, then in the exciton-band region located closer to $k = 0$ there can develop an inverse distribution of the excitons relative to the L0-phonon band, i.e., $n(k) > \nu(k_0)$ at $|k| < |k_0|$. In this case, a strong induced luminescence should be observed near the red boundary of the exciton-phonon spectrum. Such a luminescence is indeed observed at laser-radiation exciting powers 2 MW/cm^2 and above. Figure 6 shows the results of microphotometry of the intensity distribution in the luminescence spectra of CdSe single crystals at $T = 93^\circ\text{K}$, excited by ruby-laser emission. Figure 6 shows the position of the red boundary of the exciton-phonon spectrum at the same temperature. We note that the red boundary of the luminescence spectrum experiences a certain shift towards lower energies. This, as shown by estimates, may be connected with the heating of the crystal when the excitation power from the laser is large. A characteristic feature of the obtained spectrum distributions is that the maximum of the luminescence is located near the red boundary of the exciton-phonon spectrum. This is evidence of a strong concentration of the excitons near the center of the band. Clearly, such a distribution of the excitons in the band may develop in the case of a sufficiently rapid rate of intraband relaxation. Thus, the investigation of the luminescence under saturation conditions offers evidence in favor of the integral mechanism. It should be noted that in these investigations, a noticeable luminescence was observed at excitation powers exceeding the powers at which the saturation parameters are determined.

Rev. 119, 570 (1960).

¹⁴R. E. Dietz, J. J. Hopfield, and D. G. Thomas, J. Appl. Phys. 32, 2282 (1961).

¹⁵D. T. F. Marple, Phys. Rev. 150, 728 (1966).

¹⁶A. Hadni, J. Claudel, and P. Strimer, Phys. Stat. Solidi 26, 241 (1967).

¹⁷W. P. Dumke, Phys. Rev. 108, 1419 (1957).

¹⁸G. G. Macfarlane, T. P. McLean, J. E. Quarrington,

and V. Roberts, Phys. Rev. 111, 1245 (1958).

¹⁹I. S. Gorban', V. B. Timofeev, and E. F. Frolova, Fiz. Tverd. Tela 5, 977 (1963) [Sov. Phys.-Solid State 5, 711 (1963)].

Translated by J. G. Adashko
55